Supplementary Material (ESI) for Dalton Transactions
This journal is © The Royal Society of Chemistry

The Various Architectures and Properties of a Series of Coordination Polymers Tuned by the Central Metals

Xiu-Li Wang, * Jian Luan, Hong-Yan Lin, Mao Le, Guo-Cheng Liu

Department of Chemistry, Bohai University, Liaoning Province Silicon Materials Engineering Technology Research Centre, Jinzhou 121000, P. R. China

Table S1. Selected bond distances (Å) and angles (°) for complex **1**

Co(1)-N(1)	2.174(2)	Co(2)-N(2)	2.237(3)
Co(1)-N(1)#1	2.174(2)	Co(2)-N(2)#2	2.237(3)
Co(1)-O(1W)	2.0877(18)	Co(2)-O(1)	2.0889(18)
Co(1)-O(1W)#1	2.0877(18)	Co(2)-O(1)#2	2.0889(18)
Co(1)-O(2W)	2.0599(19)	Co(2)-O(3W)	2.066(2)
Co(1)-O(2W)#1	2.0599(19)	Co(2)-O(3W)#2	2.066(2)
O(2W)-Co(1)-O(2W)#1	180	O(3W)-Co(2)-O(3W)#2	180
O(2W)-Co(1)-O(1W)	90.67(8)	O(3W)-Co(2)-O(1)	88.86(8)
O(2W)#1-Co(1)-O(1W)	89.33(8)	O(3W)#2-Co(2)-O(1)	91.14(8)
O(2W)-Co(1)-O(1W)#1	89.33(8)	O(3W)-Co(2)-O(1)#2	91.14(8)
O(2W)#1-Co(1)-O(1W)#1	90.67(8)	O(3W)#2-Co(2)-O(1)#2	88.86(8)
O(1W)-Co(1)-O(1W)#1	179.999(1)	O(1)-Co(2)-O(1)#2	180
O(2W)-Co(1)-N(1)	93.37(9)	O(3W)-Co(2)-N(2)	89.49(10)
O(2W)#1-Co(1)-N(1)	86.63(9)	O(3W)#2-Co(2)-N(2)	90.51(10)
O(1W)-Co(1)-N(1)	89.40(9)	O(1)-Co(2)-N(2)	91.32(9)
O(1W)#1-Co(1)-N(1)	90.60(9)	O(1)#2-Co(2)-N(2)	88.68(9)
O(2W)-Co(1)-N(1)#1	86.63(9)	O(3W)-Co(2)-N(2)#2	90.51(10)
O(2W)#1-Co(1)-N(1)#1	93.37(9)	O(3W)#2-Co(2)-N(2)#2	89.49(10)
O(1W)-Co(1)-N(1)#1	90.60(9)	O(1)-Co(2)-N(2)#2	88.68(9)

* Corresponding author. Tel.: +86-416-3400158

E-mail address: wangxiuli@bhu.edu.cn (X.-L. Wang)

O(1W)#1-Co(1)-N(1)#1	89.40(9)	O(1)#2-Co(2)-N(2)#2	91.32(9)
N(1)-Co(1)-N(1)#1	180.00(5)	N(2)-Co(2)-N(2)#2	180
Symmetry code: #1 −x + 2, −y + 1, −z − 1; #2 −x, −y + 1, −z			

Table S2. Selected bond distances (Å) and angles (^{o}) for complex **2**

Ni(1)-O(1W)#1	2.0387(19)	Ni(2)-O(3W)#2	2.038(2)
Ni(1)-O(1W)	2.0387(19)	Ni(2)-O(3W)	2.038(2)
Ni(1)-O(2W)	2.0567(18)	Ni(2)-O(1)#2	2.0595(19)
Ni(1)-O(2W)#1	2.0567(18)	Ni(2)-O(1)	2.0595(19)
Ni(1)-N(1)#1	2.121(2)	Ni(2)-N(2)#2	2.183(3)
Ni(1)-N(1)	2.121(2)	Ni(2)-N(2)	2.183(3)
O(1W)-Ni(1)-O(1W)#1	180.00(12)	O(3W)-Ni(2)-O(3W)#2	180
O(1W)-Ni(1)-O(2W)#1	90.31(8)	O(3W)-Ni(2)-O(1)	91.66(8)
O(1W)#1-Ni(1)-O(2W)#1	89.69(8)	O(3W)#2-Ni(2)-O(1)	88.34(8)
O(1W)-Ni(1)-O(2W)	89.69(8)	O(3W)-Ni(2)-O(1)#2	88.34(8)
O(1W)#1-Ni(1)-O(2W)	90.31(8)	O(3W)#2-Ni(2)-O(1)#2	91.66(8)
O(2W)#1-Ni(1)-O(2W)	180	O(1)-Ni(2)-O(1)#2	180.00(7)
O(1W)-Ni(1)-N(1)	86.50(9)	O(3W)-Ni(2)-N(2)#2	89.61(10)
O(1W)#1-Ni(1)-N(1)	93.50(9)	O(3W)#2-Ni(2)-N(2)#2	90.39(10)
O(2W)#1-Ni(1)-N(1)	89.73(9)	O(1)-Ni(2)-N(2)#2	88.90(9)
O(2W)-Ni(1)-N(1)	90.27(9)	O(1)#2-Ni(2)-N(2)#2	91.11(9)
O(1W)-Ni(1)-N(1)#1	93.50(9)	O(3W)-Ni(2)-N(2)	90.39(10)
O(1W)#1-Ni(1)-N(1)#1	86.50(9)	O(3W)#2-Ni(2)-N(2)	89.61(10)
O(2W)#1-Ni(1)-N(1)#1	90.27(9)	O(1)-Ni(2)-N(2)	91.10(9)
O(2W)-Ni(1)-N(1)#1	89.74(9)	O(1)#2-Ni(2)-N(2)	88.89(9)
N(1)-Ni(1)-N(1)#1	179.998(1)	N(2)#2-Ni(2)-N(2)	180
Symmetry code: #1 −x, −y + 1, −z + 1; #2 −x + 2, −y + 1, −z			

Table S3. Selected bond distances (Å) and angles (°) for complex **3**

Cu(1)-O(1)#1	1.947(2)	Cu(1)-N(1)	2.000(3)
Cu(1)-O(1)	1.947(2)	Cu(1)-N(1)#1	2.000(3)
O(1)-Cu(1)-O(1)#1	180	O(1)-Cu(1)-N(1)#1	89.85(11)
O(1)-Cu(1)-N(1)	90.15(11)	O(1)#1-Cu(1)-N(1)#1	90.15(11)
O(1)#1-Cu(1)-N(1)	89.85(11)	N(1)-Cu(1)-N(1)#1	180.000(1)
Symmetry code: #1 −x + 1/2, −y + 3/2, −z + 1			

Table S4. Selected bond distances (Å) and angles (°) for complex **4**

Zn(1)-O(1)	1.9240(14)	Zn(1)-N(1)	2.0461(16)
Zn(1)-O(3)	1.9465(13)	Zn(1)-N(2)#1	2.0755(16)
O(1)-Zn(1)-O(3)	107.92(6)	O(1)-Zn(1)-N(2)#1	112.26(7)
O(1)-Zn(1)-N(1)	121.68(7)	O(3)-Zn(1)-N(2)#1	95.47(6)
O(3)-Zn(1)-N(1)	109.61(6)	N(1)-Zn(1)-N(2)#1	106.74(6)
Symmetry code: #1 −x + 1, −y, −z + 1			

Table S5. Selected bond distances (Å) and angles (°) for complex **5**

Cd(1)-O(1)	2.2784(16)	Cd(1)-N(1)	2.3200(15)
Cd(1)-O(1W)	2.2925(14)	Cd(1)-O(5)#1	2.3538(13)
Cd(1)-O(4)	2.3037(13)	Cd(1)-O(3)	2.5293(13)
O(1)-Cd(1)-O(1W)	104.50(6)	O(4)-Cd(1)-O(5)#1	93.80(5)
O(1)-Cd(1)-O(4)	85.10(5)	N(1)-Cd(1)-O(5)#1	83.93(5)
O(1W)-Cd(1)-O(4)	92.33(5)	O(1)-Cd(1)-O(3)	137.90(5)
O(1)-Cd(1)-N(1)	135.79(6)	O(1W)-Cd(1)-O(3)	87.29(5)
O(1W)-Cd(1)-N(1)	85.59(5)	O(4)-Cd(1)-O(3)	53.71(4)
O(4)-Cd(1)-N(1)	138.21(5)	N(1)-Cd(1)-O(3)	84.51(5)
O(1)-Cd(1)-O(5)#1	84.87(6)	O(5)#1-Cd(1)-O(3)	89.21(5)
O(1W)-Cd(1)-O(5)#1	169.23(5)		
Symmetry code: #1 −x + 1, −y, −z + 1			

Table S6. Hydrogen bonding geometries (Å, °) of complexes **1**, **4**, **5**

Complex	D–H···A	D–H	H···A	D···A	D–H···A
1	O1W–H1WB···O4	0.85	1.86	2.7023	173
	O1W–H1WA···O2	0.85	1.85	2.6892	167
4	O1W–H1WA···O5	0.85	2.18	3.0119	168
	O1W–H1WB···O4	0.85	2.20	3.0340	165
5	O1W–H1WA···O2	0.85	1.99	2.8327	169

Table S7 Coordination modes of metal ions, the 3-bpah and 1,4-BDC in complexes **1**–**5**.

Complexes	Metal ions	3-bpah	Dihedral angle of two pyridyl rings (°)	M···M lengths (Å)	1,4-BDC	M···M lengths (Å)
1	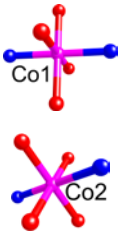	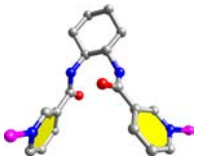	63.23	10.67	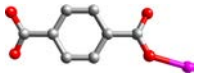	None
2	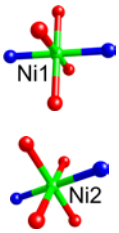	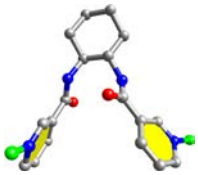	63.28	10.63	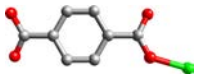	None
3		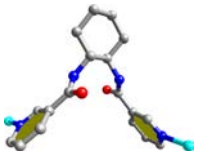	82.51	10.89		10.84
4			73.65	10.40		10.96
5		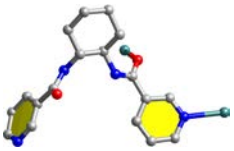	72.19	6.91	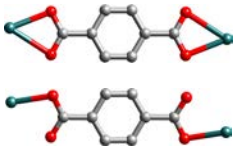	11.33 11.37

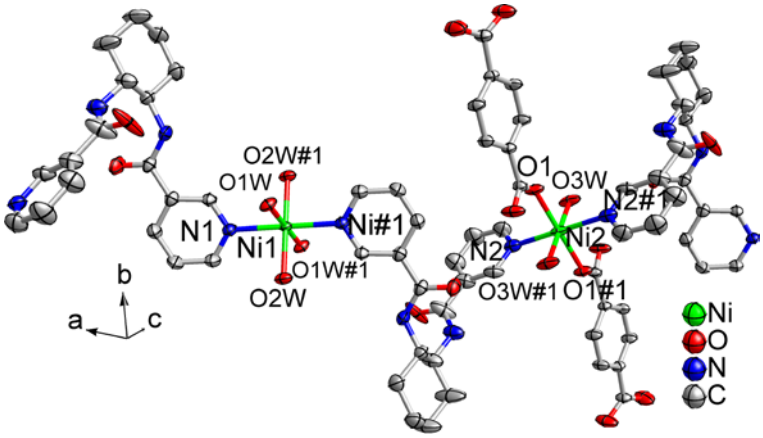

Fig. S1 The coordination environment of Ni(II) ions in complex **2** with 50% thermal ellipsoids.

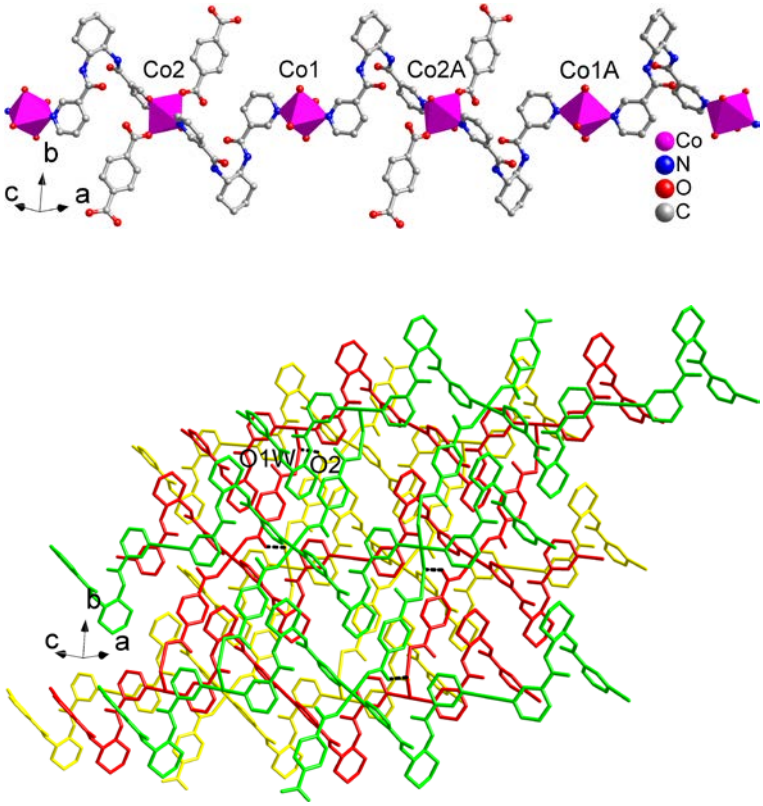

Fig. S2 (a) The 1D chain for complex **1**; (b) View of the 3D supramolecular network of complex **1**.

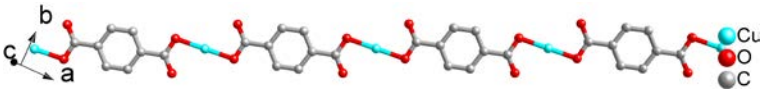

Fig. S3 View of the 1D $[Cu(1,4\text{-}BDC)]_n$ chain in complex **3**.

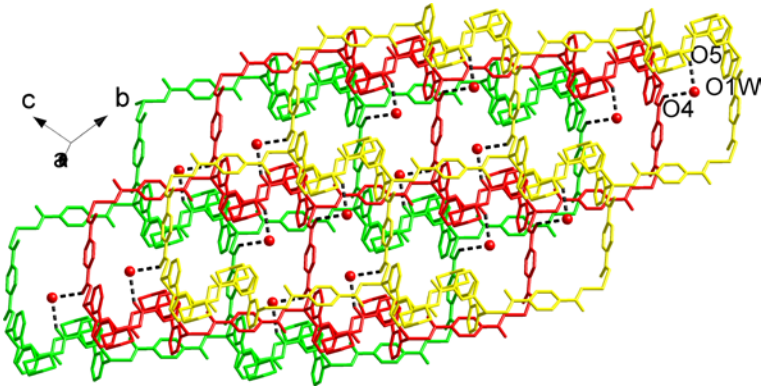

Fig. S4 View of the 3D supramolecular network of complex **4**.

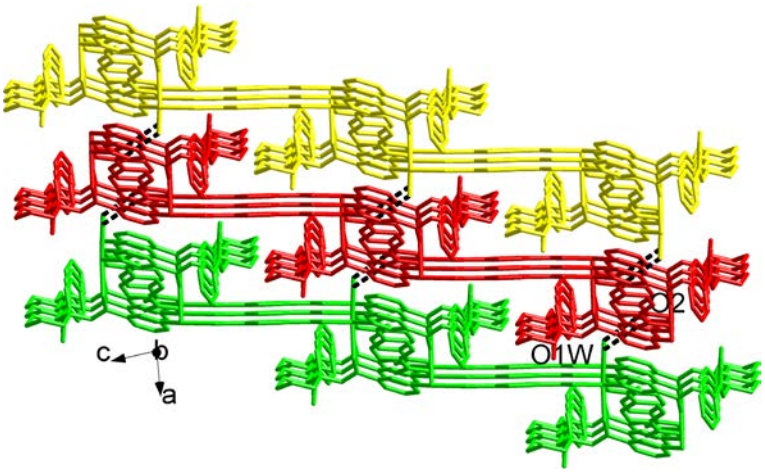

Fig. S5 View of the 3D supramolecular network of complex **5**.

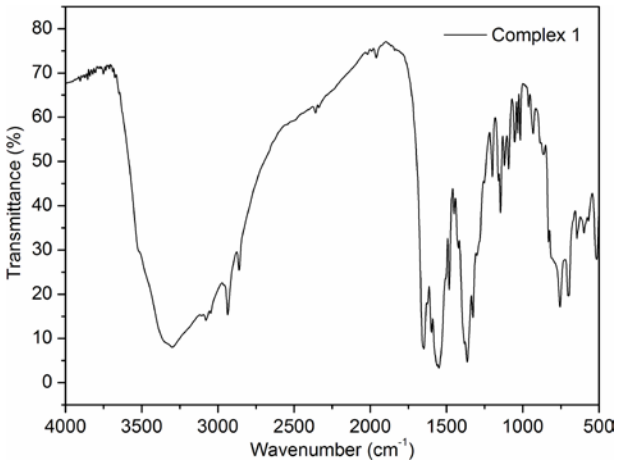

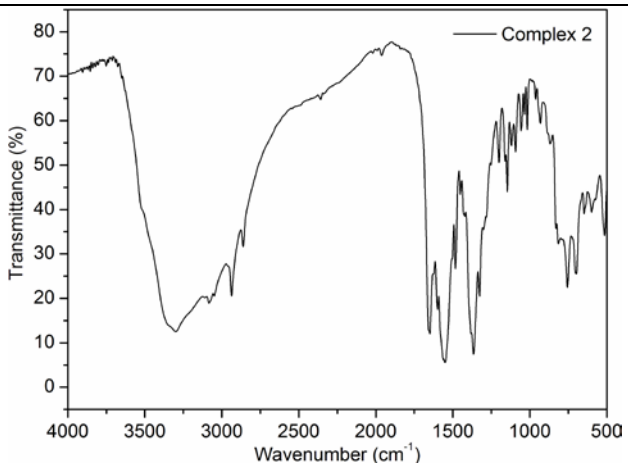
Complex 2
Transmittance (%)
Wavenumber (cm-1)

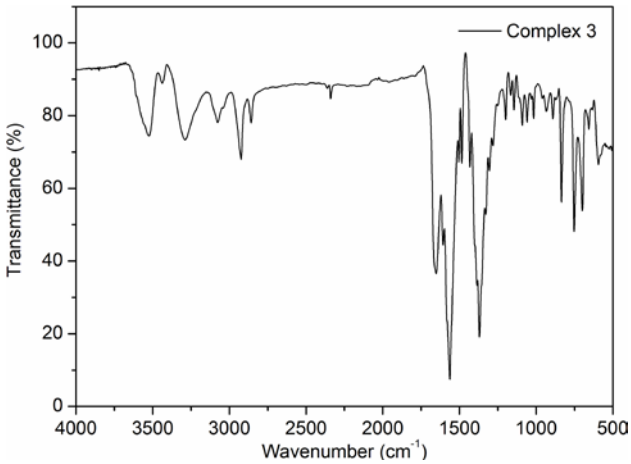
Complex 3
Transmittance (%)
Wavenumber (cm-1)

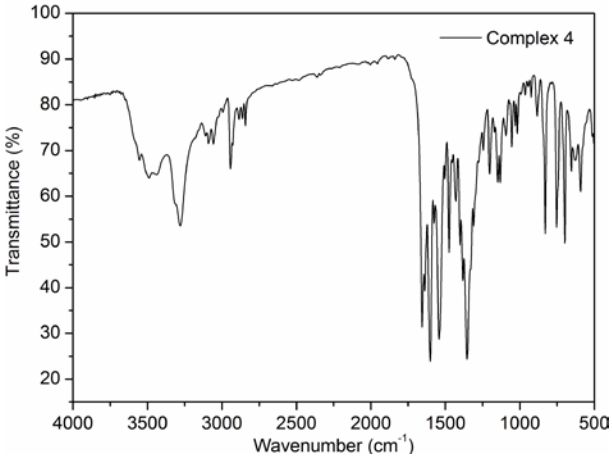
Complex 4
Transmittance (%)
Wavenumber (cm-1)

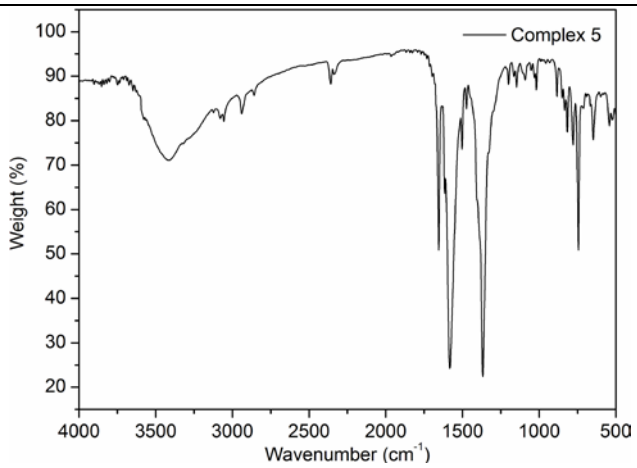

Fig. S6 The IR spectra of complexes **1**–**5**.

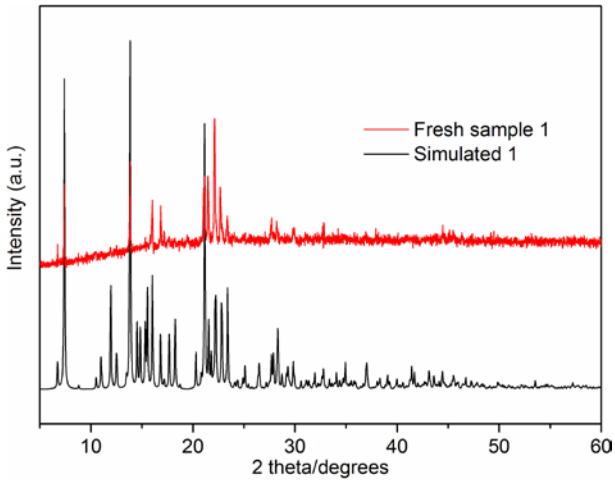

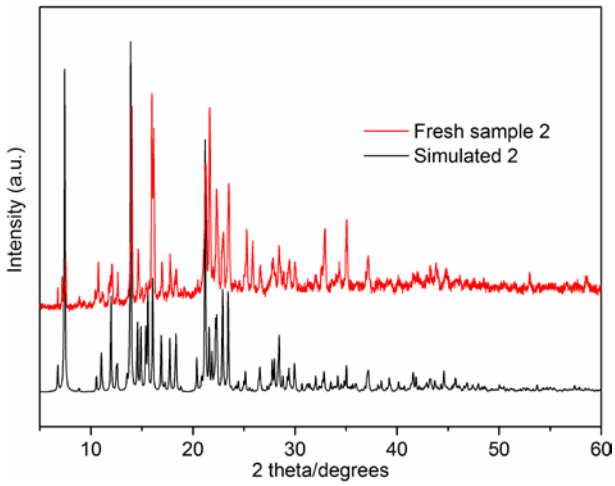

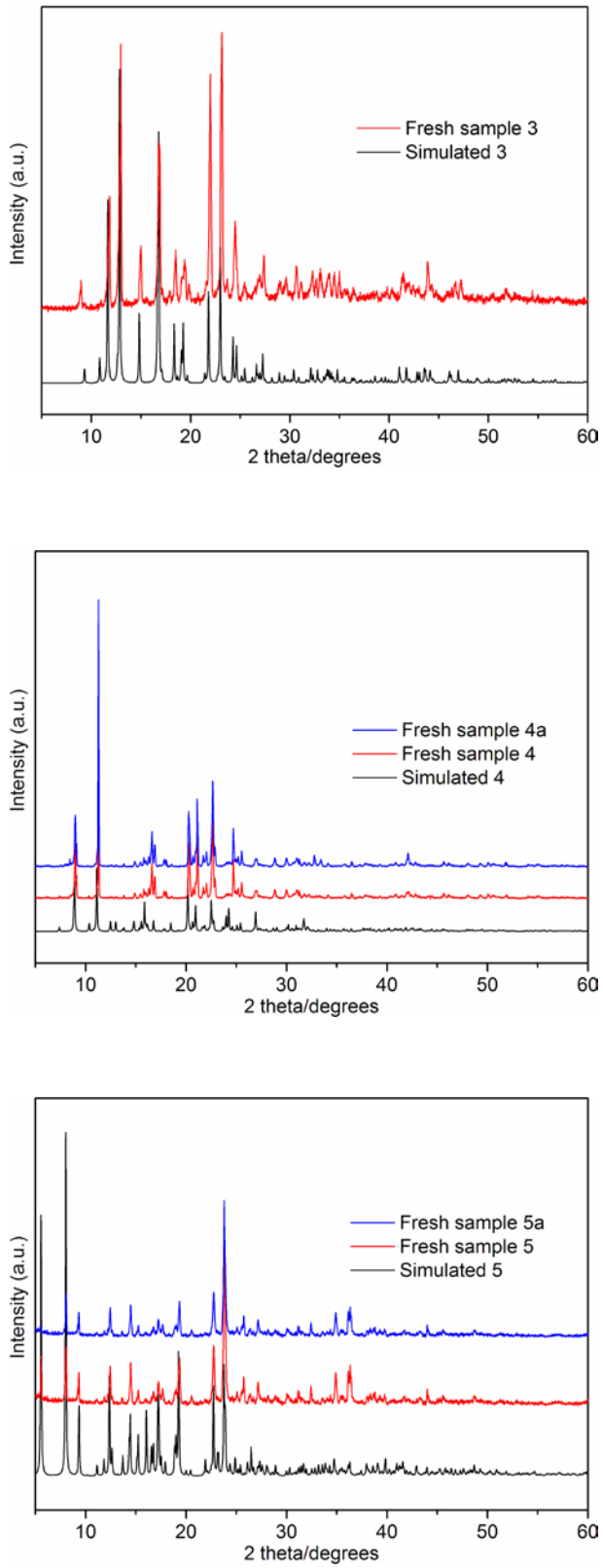

Fig.S7 The simulated (black line) and experimental (red/blue line) powder X-ray diffraction patterns for complexes **1**–**5**.

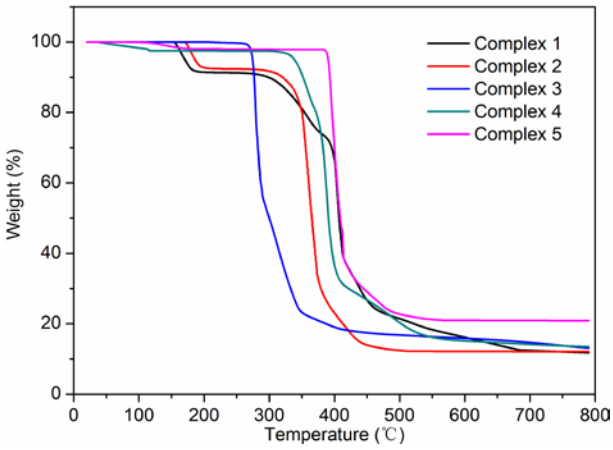

Fig. S8 The TG curves of complexes **1**–**5**.

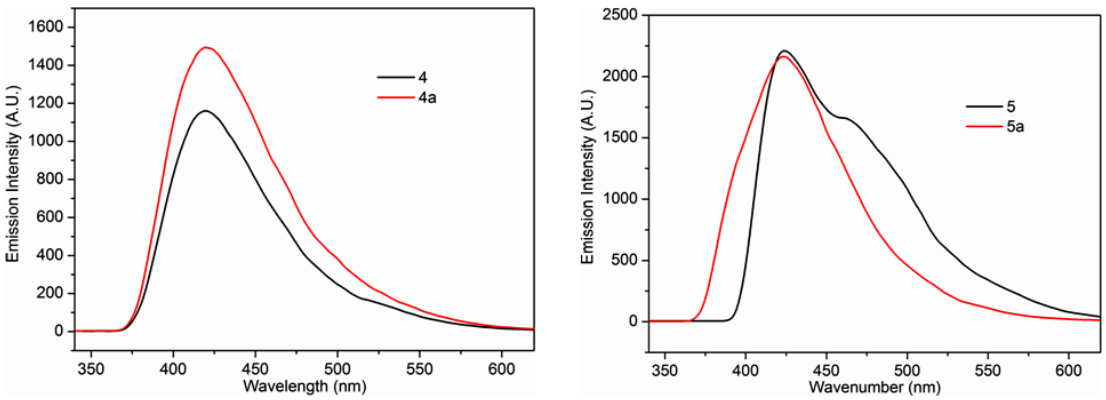

Fig. S9 The fluorescent spectra recorded on powder samples of **4a** and **5a** (the guest-free form of **4** and **5**).

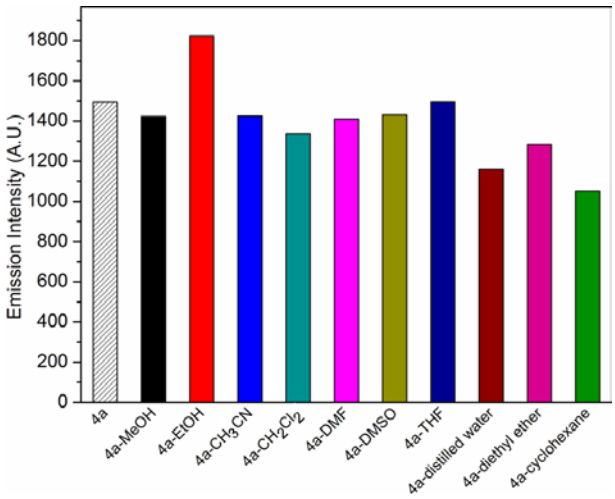

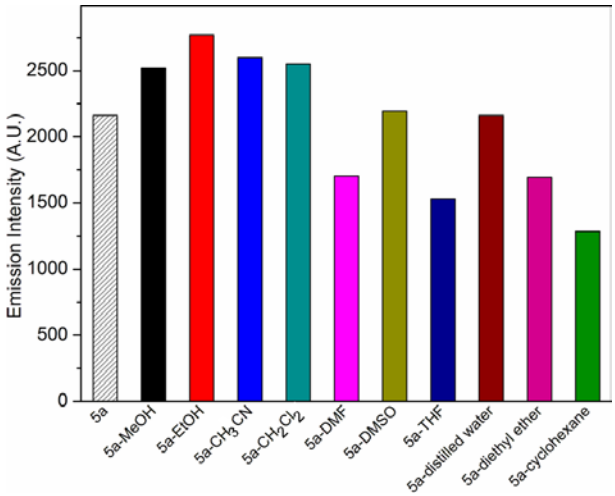

Fig. S10 Fluorescence intensity histograms of **4a**- and **5a**-solvents.

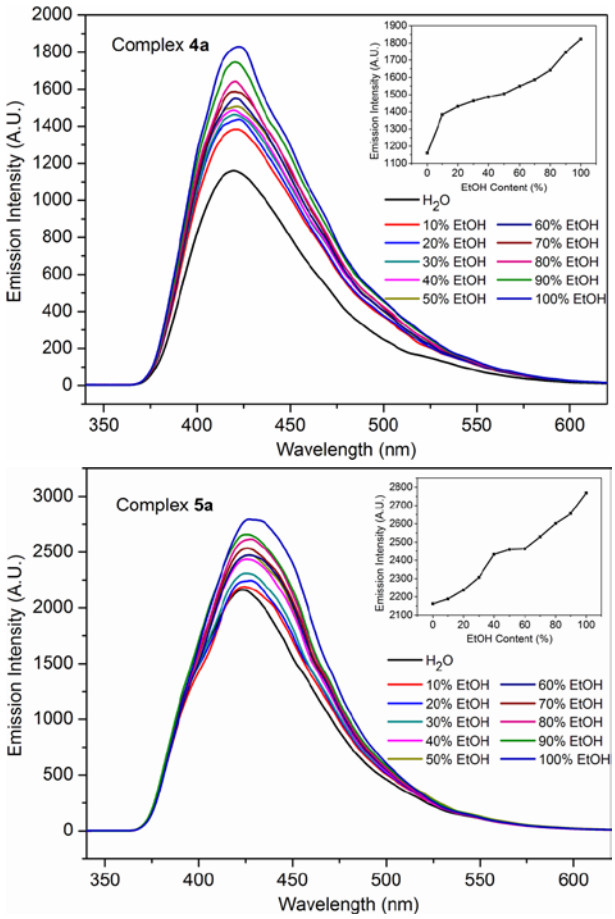

Fig. S11 The fluorescent spectra of **4a**-EtOH-H_2O and **5a**-EtOH-H_2O with various amounts of ethanol (insert is graph of the fluorescent intensity of **4a**-EtOH-H_2O and **5a**-EtOH-H_2O as a function of ethanol content).

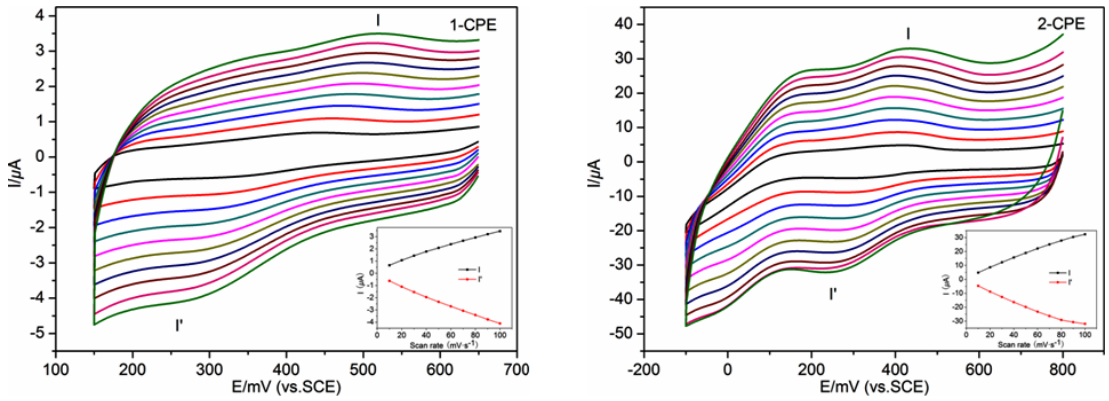

Fig. S12 Cyclic voltammograms of the **1**-CPE and **2**-CPE in 0.01 M H_2SO_4 + 0.5 M Na_2SO_4 aqueous solution at different scan rates (from inner to outer: 10, 20, 30, 40, 50, 60, 70, 80, 90, 100 mV s^{-1}), respectively. The inset shows the plots of the anodic and cathodic peak currents against scan rates.

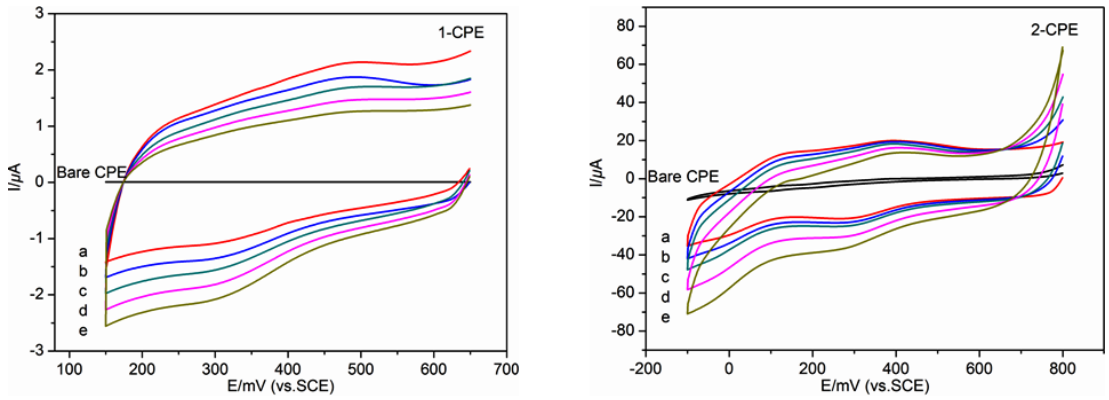

Fig. S13 Cyclic voltammograms of the bare CPE in 0.01 M H_2SO_4 + 0.5 M Na_2SO_4 aqueous solution containing 1.0 mmol/L KNO_2, **1**-CPE and **2**-CPE in 0.01 M H_2SO_4 + 0.5 M Na_2SO_4 aqueous solution containing: 0.0 (a), 2.0 (b), 4.0 (c), 6.0 (d), and 8.0 (e) mmol/L KNO_2, respectively. Scan rate: 50 mV s^{-1}.